

Exceptional service in the national interest



Magnetic Source Imaging Using a Pulsed Optically Pumped Magnetometer Array

Amir Borna, Tony R. Carter, Peter D. D. Schwindt

6th Workshop on Optically Pumped Magnetometers

August 25th, 2017

Outline

- Introduction and Motivation
- Sensor Design
- Principle of Operation
- Magnetic Imaging System
- Capturing Magnetic Signature
- 2D Magnetic Source Imaging
- Conclusion

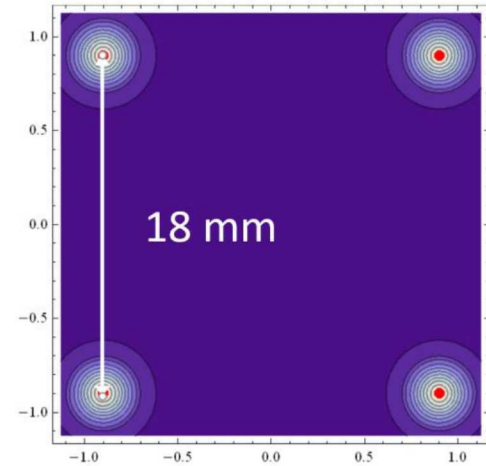
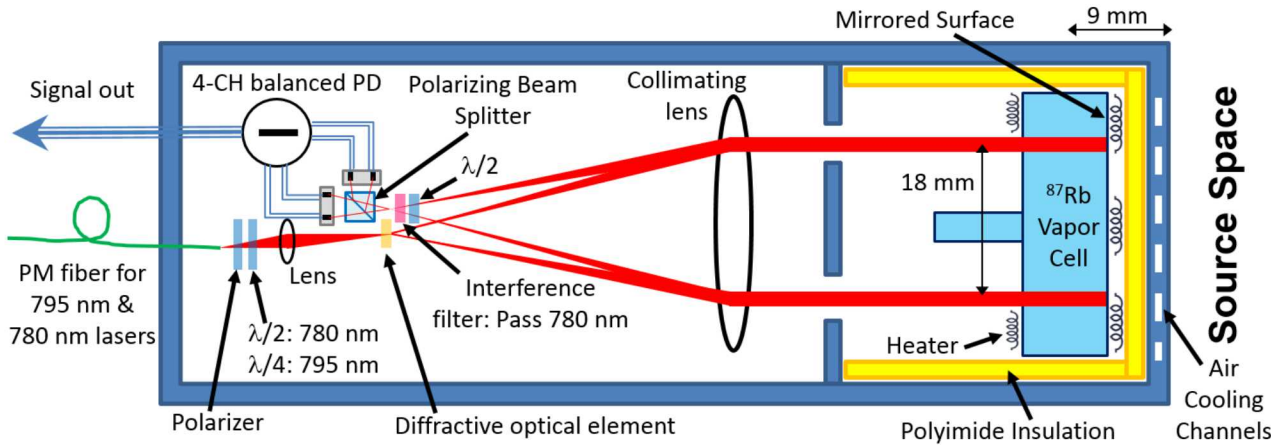
Introduction and Motivation

- Magnetic source imaging refers to reconstructing the magnetic and current dipoles underlying measured magnetic field maps.
- Magnetic source imaging has a wide range of applications such as:
 - magnetoencephalography (MEG)
 - magnetocardiography (MCG)
 - material science
 - printed-circuit-board/integrated-circuits quality-assurance
 - magnetic nanoparticle detection
- The type of magnetic sensor and its underlying sensing mechanism dictates various system level specifications including noise, dynamic range, and bandwidth.
- In the presented work, we expand the upper sensing range of our OPM sensors by operating them in pulsed-mode.

Outline

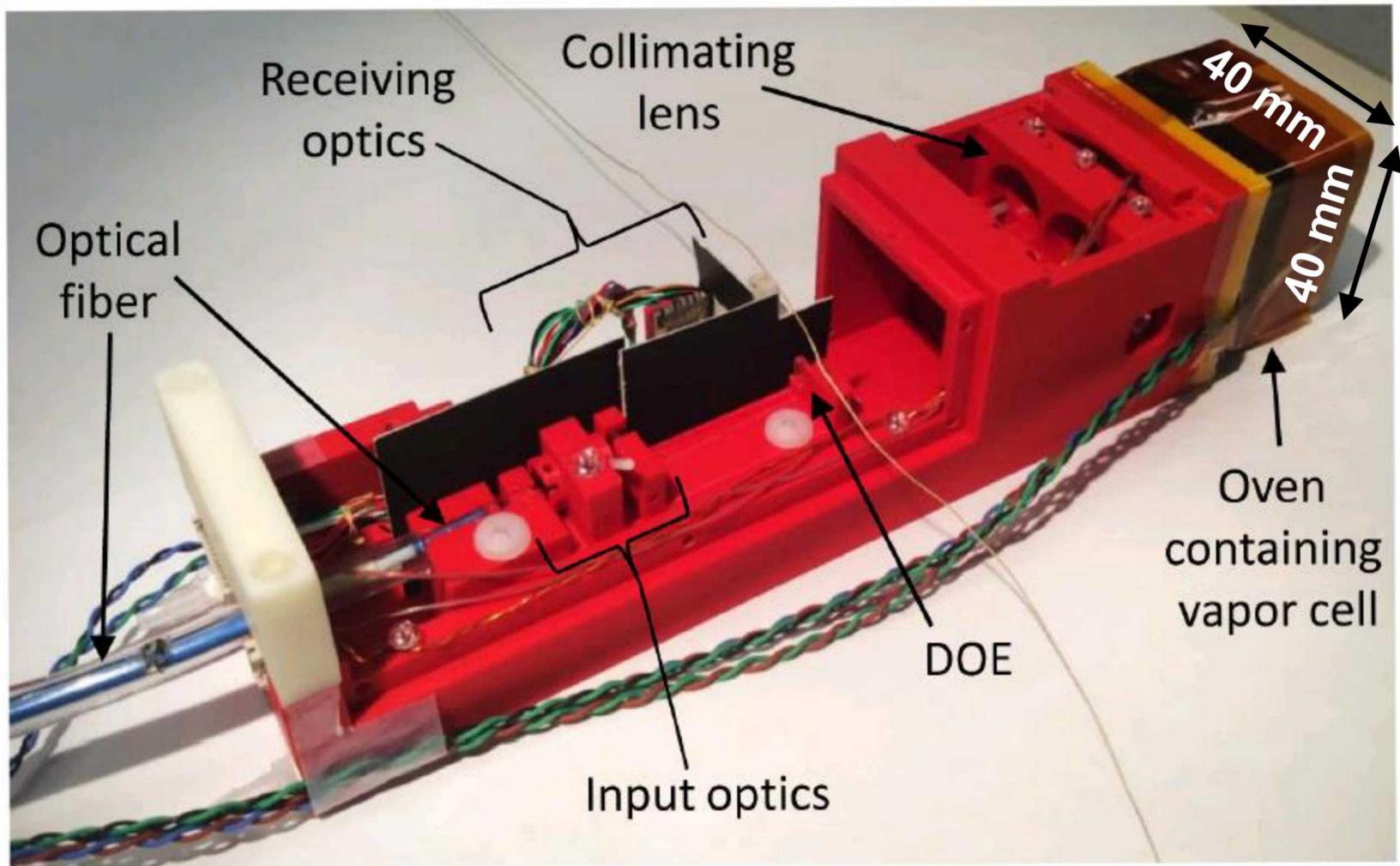
- Introduction and Motivation
- Sensor Design
- Principle of Operation
- Magnetic Imaging System
- Capturing Magnetic Signature
- 2D Magnetic Source Imaging
- Conclusion

4-Channel Sensor Design

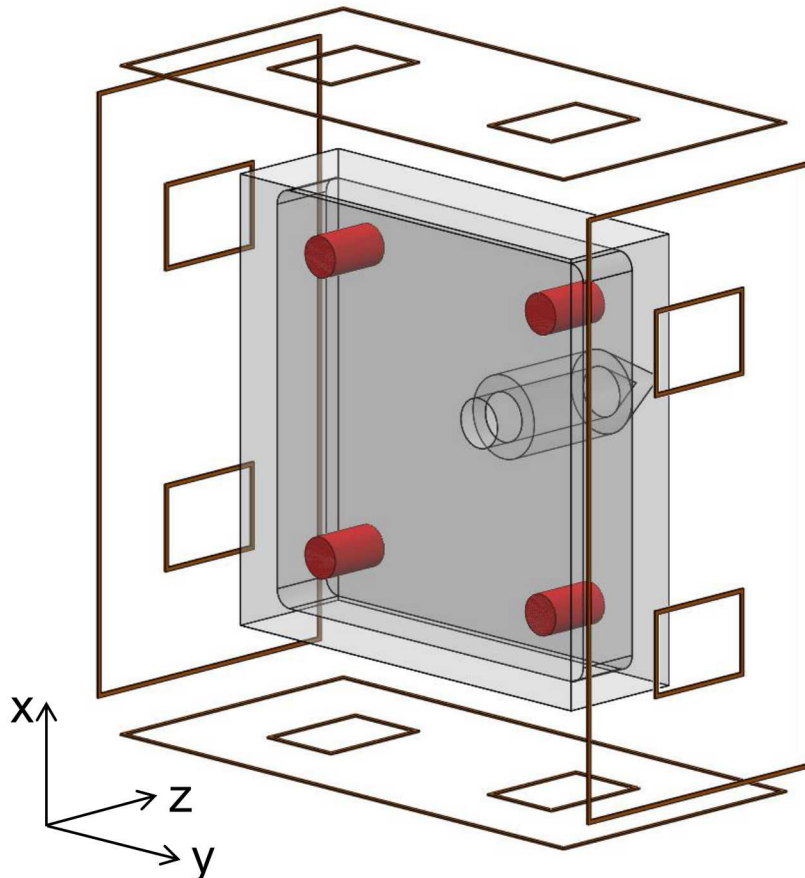


- Four separated beams:
 - 18 mm baseline
 - 2.5 mm FWHM beam diameter
- Vapor cell:
 - 4 mm long
 - 600 Torr N_2
- Sensing volume: $4 \text{ mm} \times \pi \times (1.25 \text{ mm})^2 \approx 20 \text{ mm}^3$
- Distance from the source space to the vapor cell (sensing volume): 12 mm

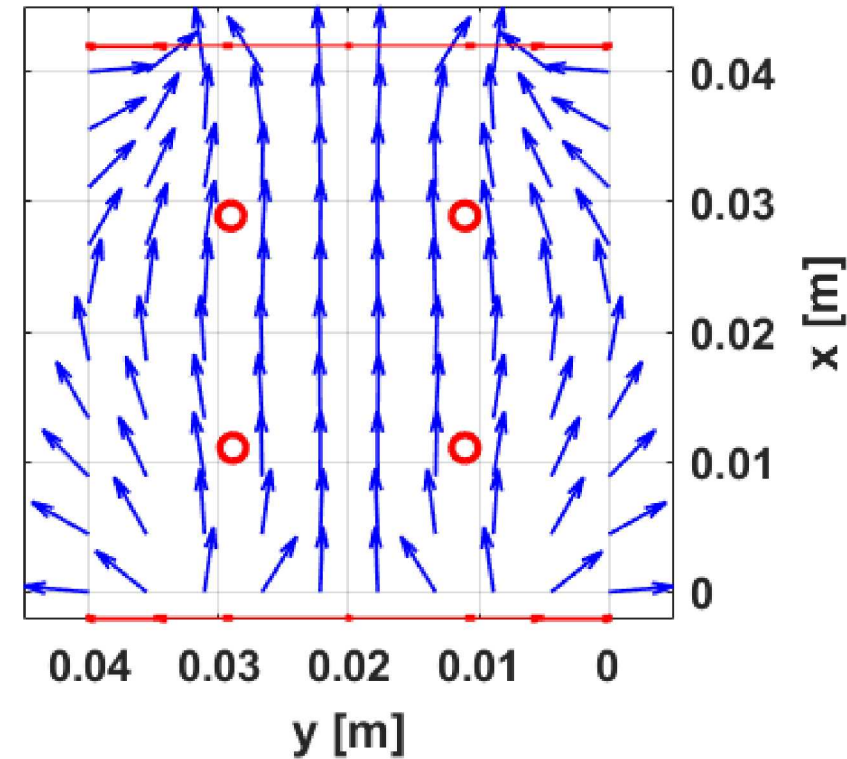
Sensor Implementation



Field Modulation and Coils



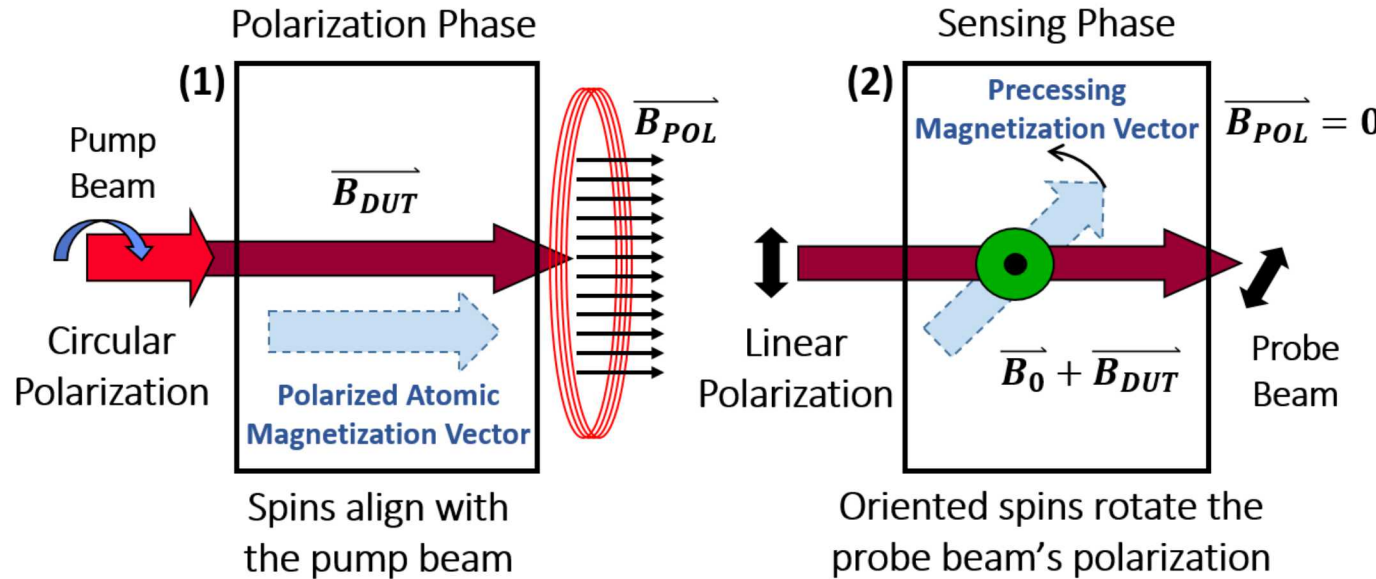
- Outer coil 18 mm x 36 mm
- Inner coils 5 mm x 7 mm



Outline

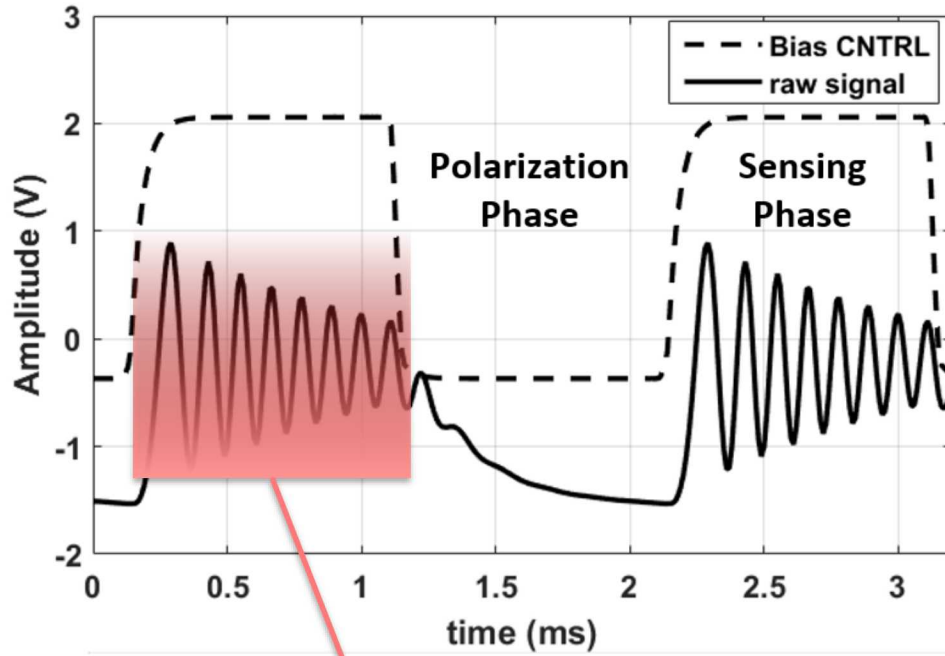
- Introduction and Motivation
- Sensor Design
- Principle of Operation
- Magnetic Imaging System
- Capturing Magnetic Signature
- 2D Magnetic Source Imaging
- Conclusion

Principle of Operation



- The Pulsed-OPM makes a **scalar** measurement of the magnitude of the total magnetic field.
- **Polarization phase:**
 - A magnetic field ($\overrightarrow{B_{POL}}$) is applied parallel to the propagation axis of the pulsed, circularly polarized pump laser.
 - The pump laser optically pumps the atomic spins parallel to the propagation axis. $\overrightarrow{B_{POL}}$ is generated by on-sensor coils and is approximately 840 nT.
- **Sensing phase:**
 - Both the pump laser and $\overrightarrow{B_{POL}}$ are turned off, and a large bias field ($\overrightarrow{B_0}$) is applied, around which the atoms precess.

Principle of Operation



$$f(t) = A_1 e^{-t/T_1} + A_2 e^{-t/T_2} \cos(2\pi f_0 t + \varphi_0) + n(t)$$

- The raw waveform of a single channel (solid line), and the control signal for the bias field, \vec{B}_0 (dashed line); the magnitude of the magnetic field during the sensing phase is proportional to the frequency of the decaying sinusoid.
- The extracted frequency is converted into magnitude of the sensed magnetic flux density ($|B|$) using the gyromagnetic ratio (γ) of the rubidium (^{87}Rb) atoms (7 Hz/nT).

$n(t)$: noise

A_1 : longitudinal polarization amplitude

A_2 : transverse polarization amplitude

T_1/T_2 : longitudinal/tangential relaxation times

φ_0 : phase of the decaying sinusoid

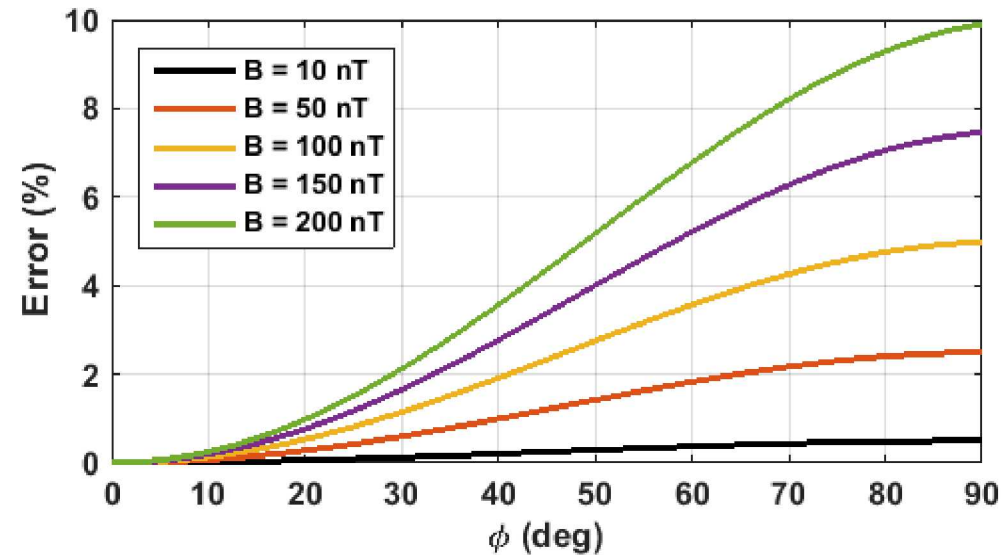
f_0 : Larmor precession frequency

Principle of Operation

- The large bias magnetic field is set to $\sim 1 \mu\text{T}$, and assuming it is much larger than the magnetic field contributed by the device under test ($|\overrightarrow{B_0}| \gg |\overrightarrow{B_{DUT}}|$), the extracted magnetic field can be expressed as:

$$|\overrightarrow{B_{OPM}}| = \sqrt{|\overrightarrow{B_{DUT,x}}|^2 + |\overrightarrow{B_{DUT,y}} + \overrightarrow{B_{0,y}}|^2 + |\overrightarrow{B_{DUT,z}}|^2} \approx \sqrt{|\overrightarrow{B_{DUT,y}} + \overrightarrow{B_{0,y}}|^2} = |\overrightarrow{B_{DUT,y}} + \overrightarrow{B_{0,y}}|$$

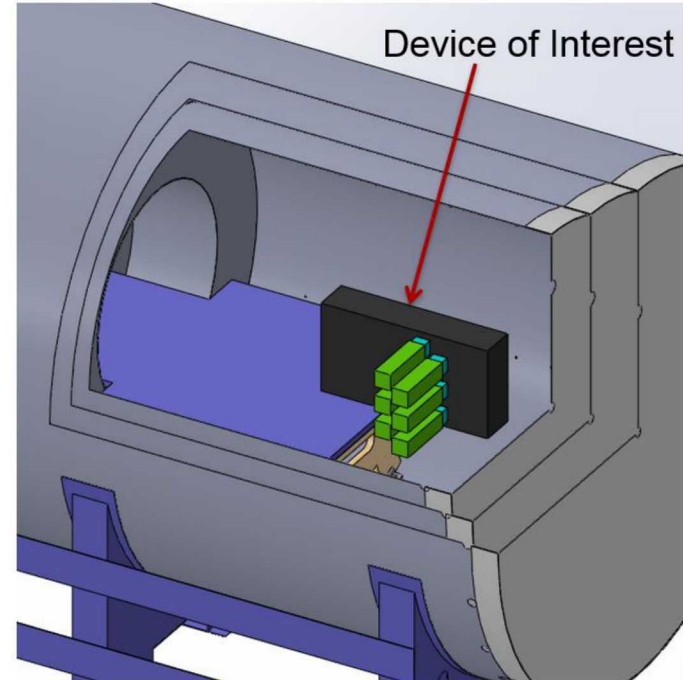
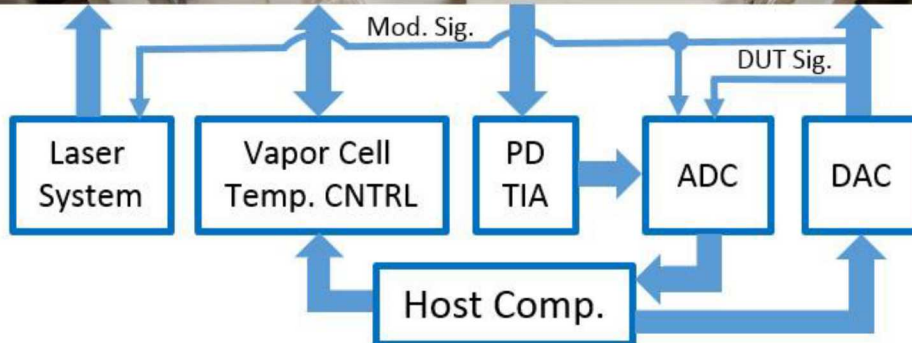
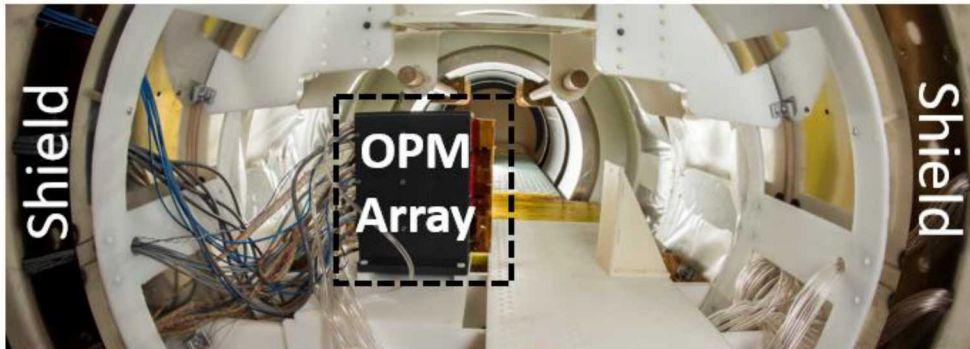
- The validity of above equation, depends on the ratio of $|\overrightarrow{B_{DUT}}|/|\overrightarrow{B_0}|$ and the angle between $\overrightarrow{B_0}$ and $\overrightarrow{B_{DUT}}$.
- Calculated error of the pulsed-OPM magnetic imaging system; the bias field is $1 \mu\text{T}$; ϕ is the angle between the sensed magnetic field ($\overrightarrow{B_{DUT}}$) and the bias field ($\overrightarrow{B_0}$).



Outline

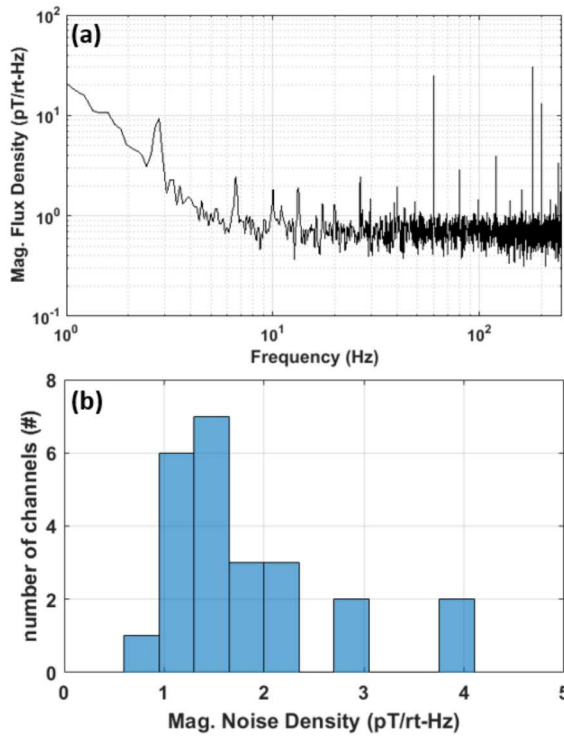
- Introduction and Motivation
- Sensor Design
- Principle of Operation
- Magnetic Imaging System
- Capturing Magnetic Signature
- 2D Magnetic Source Imaging
- Conclusion

Magnetic Imaging System

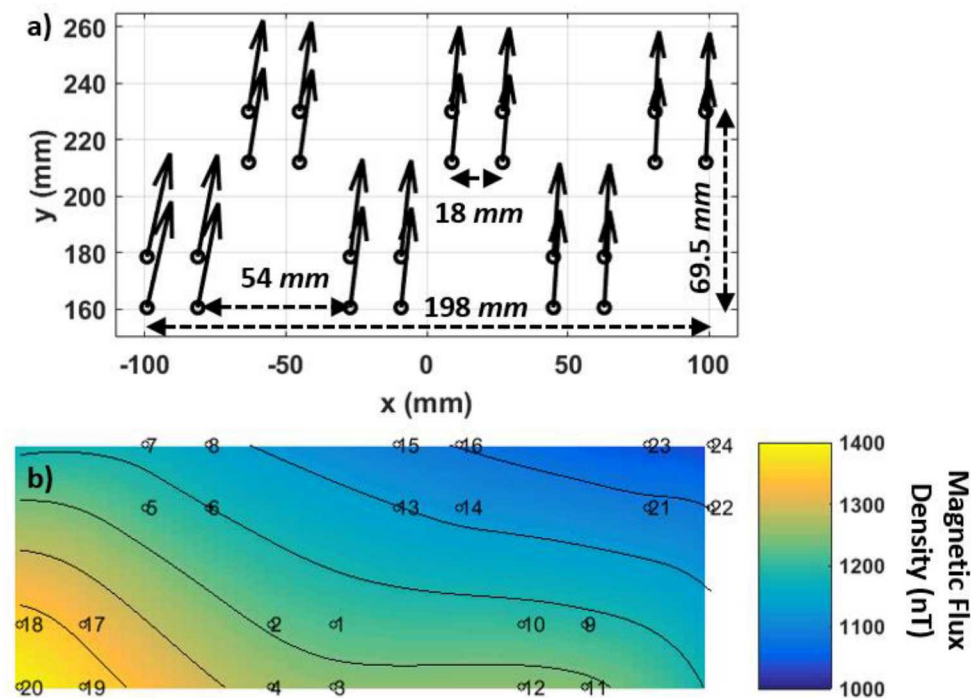


- The magnetic sensor array inside the three-layer magnetic shield.
 - PD TIA: transimpedance amplifiers of the photo diodes;
 - ADC: analog-to-digital-converter;
 - DAC: digital-to-analog-converter;
 - DUT Sig.: the signal driving the device under test;
 - Mod. Sig.: the control signal modulating the laser system, the bias field, and the polarizing magnetic field.

Magnetic Imaging System



The noise spectrum of the pulsed OPM sensor (a) and the 24-channel array noise floor histogram (b).



The vector field map of the bias magnetic field measured by a commercial fluxgate magnetometer (a), and the bias magnetic field's magnitude measured by the presented OPM array (b). The array's dimensions are indicated on the fluxgate vector field map (a).

Magnetic Imaging System

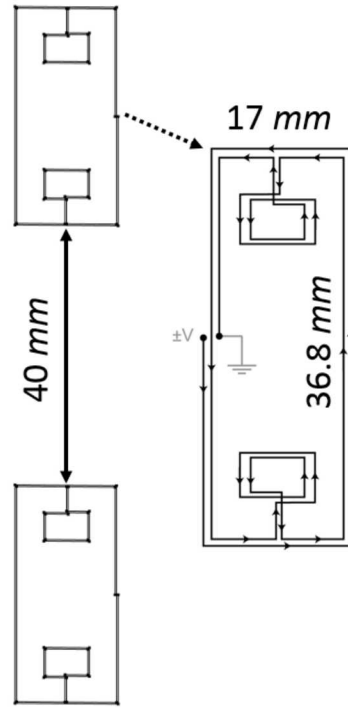
PERFORMANCE SUMMARY OF MAGNETIC SENSORS

	Noise	Upper Sensing Range	3 dB Bandwidth	Operating Temperature	Magnetic Shielding	Principle of Operation
Bell-Bloom [31]	$0.1\text{-}5 \text{ pT}/\sqrt{\text{Hz}}$	$\pm 10 \text{ }\mu\text{T}$	0.5-10 kHz	20-120 °C	No	Electron Spin Precession
M_x [30]	$0.1\text{-}5 \text{ pT}/\sqrt{\text{Hz}}$	$\pm 10 \text{ }\mu\text{T}$	0.5-10 kHz	20-120 °C	No	Electron Spin Precession
Pulsed-OPM [this work]	$0.1\text{-}5 \text{ pT}/\sqrt{\text{Hz}}$	$\pm 10 \text{ }\mu\text{T}$	0.5-2 kHz	120 °C	No	Electron Spin Precession
SERF [19]	$0.2\text{-}10 \text{ fT}/\sqrt{\text{Hz}}$	$\pm 5 \text{ nT}$	5-300 Hz	150-200 °C	Yes	Electron Spin Precession
Low- T_c SQUID [5]	$\sim 3 \text{ fT}/\sqrt{\text{Hz}}$	NA	$\sim 1 \text{ MHz}$	-269 °C	No	Josephson Junctions
Fluxgate [18]	$35 \text{ pT}/\sqrt{\text{Hz}}$	$\pm 60 \text{ }\mu\text{T}$	3.5 kHz	Room Temp.	No	Sat. of Ferromagnetic Materials
GMR [17]	$0.2 \text{ nT}/\sqrt{\text{Hz}}$	7 mT	1 MHz	Room Temp.	No	Spin-Dependent Scattering
Hall Effect [10, 11]	$30 \text{ nT}/\sqrt{\text{Hz}}$	7 mT	120 kHz	Room Temp	No	Lorentz Force

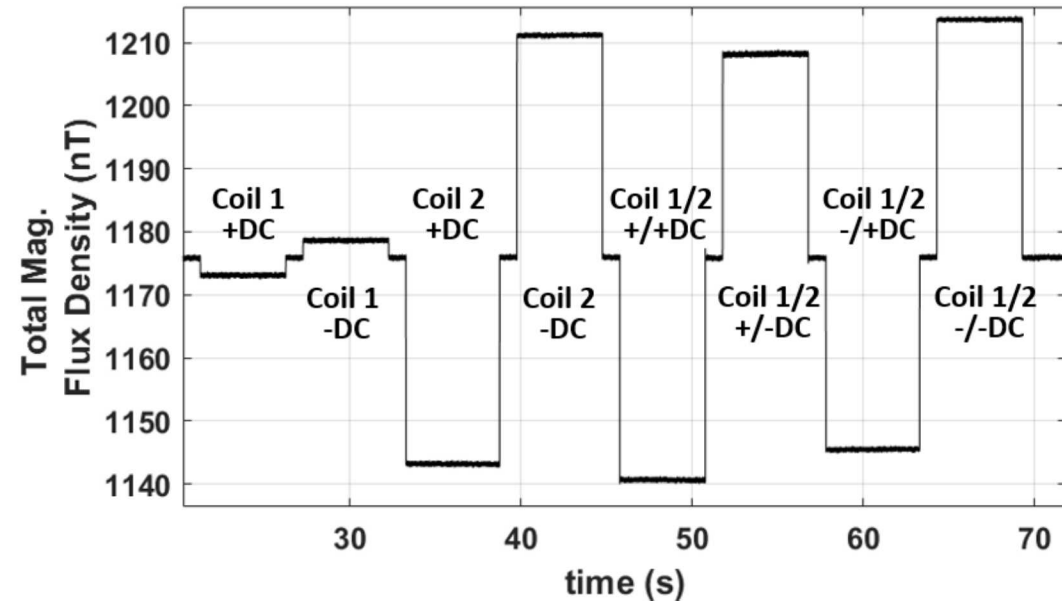
Outline

- Introduction and Motivation
- Sensor Design
- Principle of Operation
- Magnetic Imaging System
- Capturing Magnetic Signature
- 2D Magnetic Source Imaging
- Conclusion

Capturing Magnetic Signature

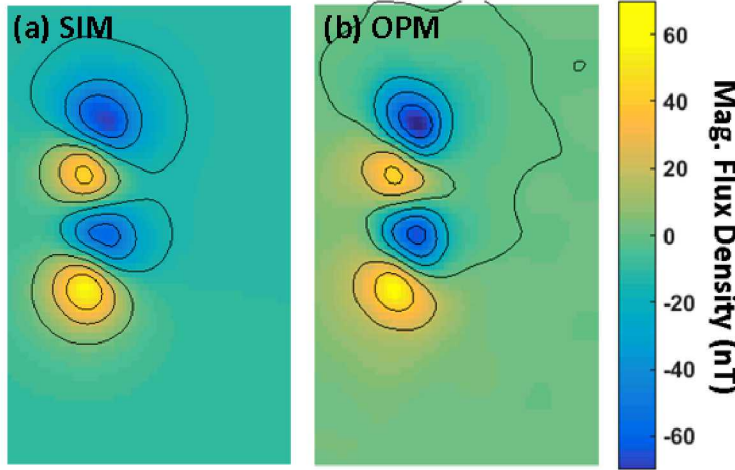


Device under test (DUT)
coil structure

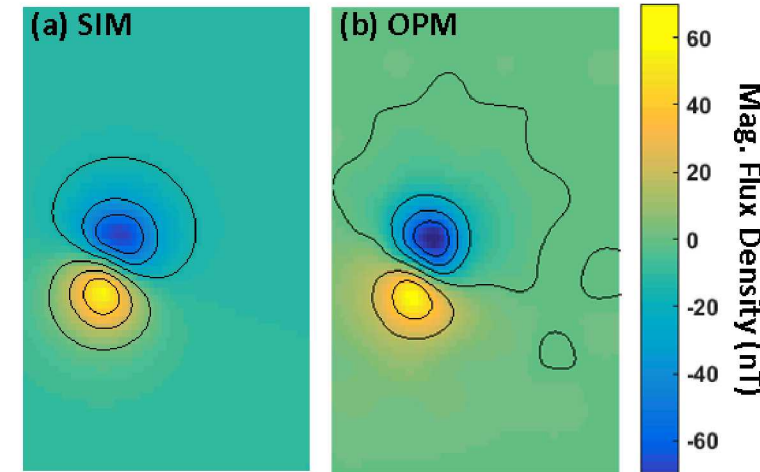


Time domain waveform of a measured pulsed-OPM channel when current is applied to the coils in the test structure

Capturing Magnetic Signature



Double Coil DC field map simulation (a), and the measured field map using the pulsed-OPM array (b).

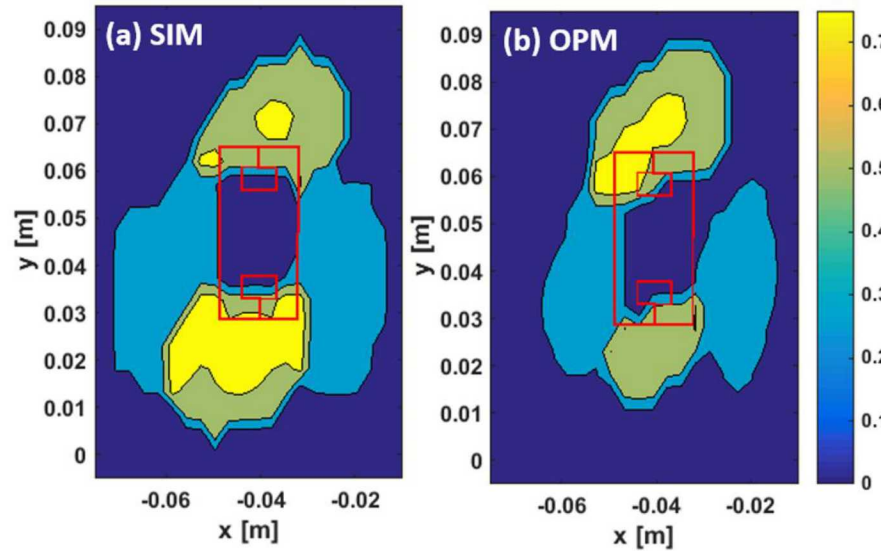


Single Coil DC field map simulation (a), and the measured field map using the pulsed-OPM array (b).

Outline

- Introduction and Motivation
- Sensor Design
- Principle of Operation
- Magnetic Imaging System
- Capturing Magnetic Signature
- 2D Magnetic Source Imaging
- Conclusion

2D Magnetic Source Imaging



Current distribution imaging using simulated (a) and measured (b) magnetic fields at a plane to sensor distance of 2.8 cm. The coil structure is overlaid on top of the constructed current density vectors.

$$B_y(x, y, z_0) = \frac{\mu_0 d}{4\pi} z_0 \int_{-\infty}^{+\infty} \int_{-\infty}^{+\infty} \frac{J_x(x', y')}{[(x - x')^2 + (y - y')^2 + z_0^2]^{\frac{3}{2}}} dx' dy'$$

$$G(x, y, z_0) = \frac{\mu_0 d}{4\pi} z_0 \frac{1}{[x^2 + y^2 + z_0^2]^{\frac{3}{2}}}$$

$$FT2D\{G(x, y, z_0)\} = \left(\frac{\mu_0 d}{2}\right) \exp\left(-z_0 \sqrt{k_x^2 + k_y^2}\right)$$

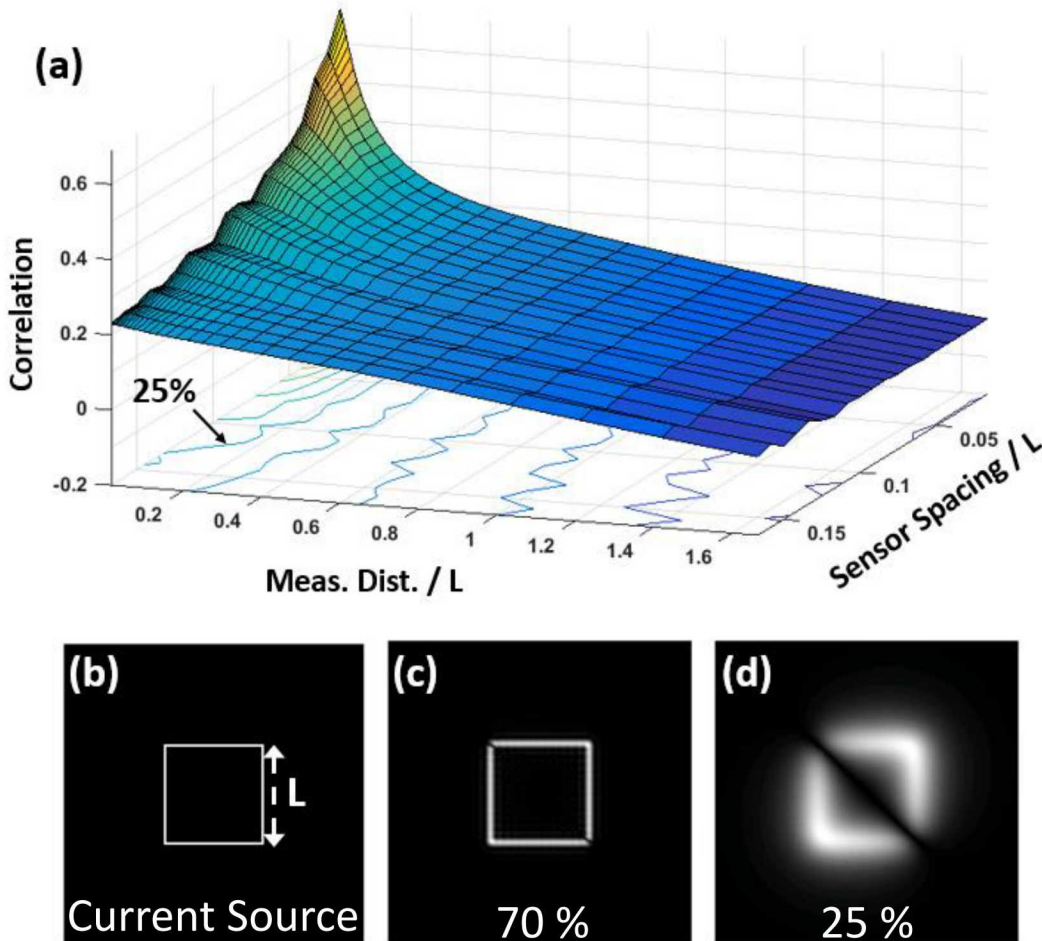
$$J_y(x, y) = FT2D^{-1} \left\{ -\frac{k_x}{k_y} \frac{FT2D\{B_y(x, y, z_0)\}}{FT2D\{G(x, y, z_0)\}} \right\}$$

$$J_x(x, y) = FT2D^{-1} \left\{ \frac{FT2D\{B_y(x, y, z_0)\}}{FT2D\{G(x, y, z_0)\}} \right\}$$

Equations Governing 2-D imaging

B. J. Roth, N. G. Sepulveda, and J. P. Wikswo, "USING A MAGNETOMETER TO IMAGE A TWO-DIMENSIONAL CURRENT DISTRIBUTION," *Journal of Applied Physics*, Article vol. 65, no. 1, pp. 361-372, Jan 1989.

2D Magnetic Source Imaging



The dependency of the constructed current density image quality on the measurement distance (z_0) and array's sensor spacing normalized to the length of the side, L : a) the correlation between the original current carrying trace and the constructed current density image; b) the 1-cm wide original current carrying trace with a side length of 30 cm; c-d) the constructed current density image for a correlation of 70 % and 25 % respectively.

Conclusion



- We have developed a pulsed optically pumped magnetometer array for magnetic sensing and current imaging applications.
- The pulsed-OPM system has a noise floor of 0.8 pT/VHz, a sampling frequency of 500 S/s (bandwidth \sim 250 Hz), and a dynamic range of 72 dB.
- By comparing the experimental results to the simulation results, we have shown the robustness of our system in capturing the magnetic signature of a general planar 2D coil structure.
- We have successfully reconstructed an image of the planar 2D coil's current density using the magnetic field map measured by the pulsed-OPM system.
- Future Work:
 - Improving noise performance by reducing the bias generator circuitry noise.
 - Expanding the source space to 3D by implementing beamforming algorithm on the measured magnetic field.

Acknowledgements

- **Sandia MEG Team:** Peter Schwindt, Amir Borna, Anthony Colombo, Yuan-Yu Jau, Tony Carter.
- **Former Team Members:** Amber Dagel, Christopher Berry, Cort Johnson, George Burns, Jon Bryan, Grant Biedermann, Michael Pack, Aaron Hankin
- **Funding:** NA-22



Sandia National Laboratories is a multimission laboratory managed and operated by National Technology and Engineering Solutions of Sandia, LLC, a wholly owned subsidiary of Honeywell International, Inc., for the U.S. Department of Energy's National Nuclear Security Administration under contract DE-NA0003525.